

NUMERICAL STUDY OF A CIRCULATOR USING YIG THIN FILM WITH A COPLANAR STRUCTURE

O. Zahwe, B. Sauviac, B. A. Samad, J. P. Chatelon
and J.-J. Rousseau

DIOM Laboratory

TELECOM Saint-Etienne, École Associée de l'Institut TELECOM
Université de Saint-Etienne, F-42000, Saint-Etienne, France
Université de Lyon, F-69000, Lyon, France

Abstract—The transmission characteristics of a high frequency circulator, using coplanar waveguides, have been designed and studied. To miniaturize the device, we have dramatically reduced the thickness of the YIG (Yttrium Iron Garnet) ferrite layer. The circulator has a hexagonal shape with dimensions of $10 \times 10 \text{ mm}^2$; the width of the central line (LINE) is $400 \mu\text{m}$; the space between LINE-to-GND is $130 \mu\text{m}$ and the thickness of the YIG film is $10 \mu\text{m}$. This compact circulator operates at 10 GHz. The insertion loss is 3.14 dB; the return loss is 18.57 dB and the isolation is greater than 20 dB.

1. INTRODUCTION

This paper deals with the field of passive microwave components. Coming from the requirements of mobile communication devices, miniaturization of microwave components is needed. The DIOM laboratory is using the RF sputtering to realize magnetic thin films. The use of these magnetic thin films for a circulator design enables to develop a new manufacturing technique compatible with the miniaturization of these devices. These components are devoted to future wireless applications in the 8–12 GHz frequency range. The advantages of these components lie in using YIG thin film and in the fact that accesses to the device are coplanar waveguide (CPW). The CPW structure has a signal line and a ground in the same plane. Therefore, the circulator with a CPW structure will be easily fabricated using low cost lithography. Moreover, connections with other devices will be easier.

Corresponding author: O. Zahwe (oussama.zahwe@univ-st-etienne.fr).

Usually, circulators are designed according to some approximate rules which are well-known but are specific to stripline circulators. As a result, for a coplanar circulator, an optimization of the initial design must be performed before obtaining a functional device. These rules will be presented first. The design and S -parameters are based on the theoretical results obtained from a stripline structure [1, 2]. These outcomes are then transposed to a coplanar design after a numerical study. The CPW structure has a signal line and a ground in the same plane. Therefore, the circulator with a CPW structure will be easily fabricated using lithography process at low cost. Moreover connections with other devices are easier.

Many researchers have studied the transmission characteristics of Y-junctions stripline circulators since Bosma's work in the sixties [1, 2], but there are few papers talking about coplanar circulators. Here are some of the most significant designs that we have found in the literature:

- In 1971 Ogasawara et al. [3] fabricated a circulator with a coplanar waveguide on a ferrite substrate.
- In 1986 Koshiji et al. [4] designed a coplanar waveguide with a cylindrical ferrite post.
- In 2004–2005, Oshiro et al. [5] realized and measured a coplanar circulator with two YIG ferrite substrates (500 μm thick).

All of them employed a bulk piece of ferrite. Our objective is to prove that it is possible to make a miniature circulator with a 10 μm ferrite film only. As the manufacturing process developed in our DIOM laboratory allows making YIG thin films, then it will be possible for us to prospect for collective fabrication in order to reduce the production costs.

In this paper, specific physical parameters have been used: the YIG film has been modelled with a dielectric constant $\varepsilon_r = 15.3$, a dielectric loss tangent with a maximum of $\tan \delta = 2 \cdot 10^{-4}$ (typical values at 8.3 GHz, given by the Temex company for massive ferrite film), a saturation magnetization $M_s = 0.139 \text{ kA/m}$ and a ferromagnetic resonance (FMR) line width $\Delta H = 7.985 \text{ kA/m}$. For conductor lines made of gold, the conductivity is $\sigma = 41 \cdot 10^6 \text{ S/m}$. The ferrite is supposed to be saturated and the internal bias field is supposed to be uniform. In this analysis the permeability tensor for a soft ferrite is given by:

$$\bar{\bar{\mu}} = \mu_0 \begin{bmatrix} \mu & -j\kappa & 0 \\ j\kappa & \mu & 0 \\ 0 & 0 & 1 \end{bmatrix} \quad (1)$$

with

$$\mu = 1 + \frac{(\omega_b + i\alpha\omega)\omega_m}{(\omega_b + i\alpha\omega)^2 - \omega^2} \quad (2)$$

$$\kappa = 1 + \frac{\omega\omega_m}{(\omega_b + i\alpha\omega)^2 - \omega^2} \quad (3)$$

Where $\omega_b = \gamma H_i$ is the gyromagnetic resonance frequency, $\omega_m = \gamma M_s$ and $\alpha\omega = \gamma \Delta H/2$. Here ω is the angular frequency; H_i is the magnetic bias field (internal field); and γ is the gyromagnetic ratio.

High frequency electromagnetic simulations were done using Ansoft HFSS software which is based on the three dimensional finite elements method (FEM). In simulations, the ferrite is modelled using Polder's tensor [6] as in equation (1).

2. HIGH FREQUENCY MODELING OF THE CIRCULATOR

First, a stripline circulator is studied with the usual analytical method. The aim is to design a circulator with a YIG thin film. So, when the stripline circulator functions properly with the magnetic thin film, the effect of several parameters on the performance is evaluated using a numerical model. After an optimized design is obtained, we transform the circulator under its coplanar version and finish the study with numerical adjustments.

2.1. Analytical and Numerical Modeling of Stripline Circulator

The stripline circulator is composed of a circular inner conductor from which three 120° oriented stripline start. Above and below this inner conductor, there are two circular discs of YIG, then two ground planes are closing the structure (see Figure 1).

From the theoretical results obtained by Bosma [1, 2], design rules were achieved, resulting in possible dimensions of a functional Y-junction stripline circulator. The formulas are based on the use of Green's functions. The conditions of circulation are obtained when we consider that the magnetic field is constant at the three ports [2]. Solving the integral equation allows to obtain the main parameters of the circulator R , ψ , and W (See Figure 2).

When the design is done, simulations are realized with Ansoft HFSS software, to be sure that the theoretical dimensions are suitable for a real design.

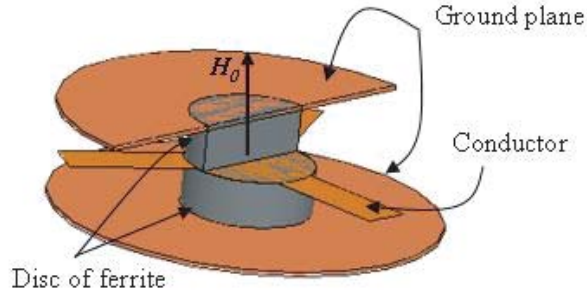


Figure 1. Y-junction stripline circulator.

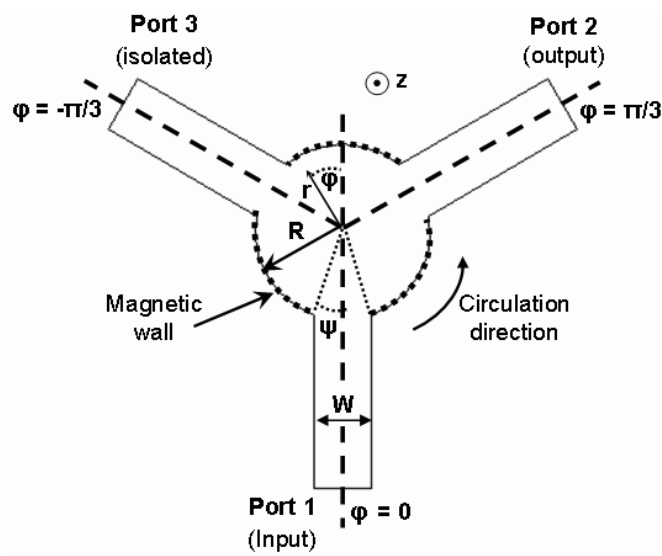


Figure 2. Configuration of the central conductor.

2.1.1. Effect of the Conductor Radius R

In his study, Bosma assumed that the radius of the ferrite is the same as one of the conductor lines ($r = R$). The radius R of ferrite disks (4) is extracted from [2].

$$X = kR = \omega \sqrt{\varepsilon \varepsilon_0 \mu_{eff} \mu_0} \quad \text{with} \quad \mu_{eff} = \frac{\mu^2 - \kappa^2}{\mu} \quad (4)$$

Where ε_0 is the free space permittivity, μ_0 is the free space permeability, ε is the relative permittivity of the ferrite and μ_{eff} is the

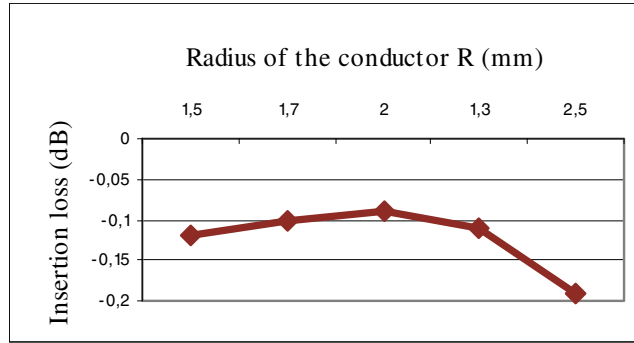


Figure 3. Numerical results for the insertion loss of the stripline circulator as a function of the radius of the conductor.

effective permeability of the ferrite derived from the elements of the magnetic Polder's tensor [6]. For the first resonance mode of the disk of ferrite, we have used the first root of the derivative of the first order Bessel function ($x = x_{1,1} = 1,84$). With the material parameters given in the introduction, we have derived the value $R = 2$ mm. Using this value, we have made a set of simulations to be sure of our optimization and modelling. The radius of the conductor has been changed from 1.5 to 2.5 mm, as shown in Figure 3. The insertion loss has reached the minimum value at R equal to 2 mm.

2.1.2. Effect of the Stripline Conductor Width W

The stripline conductor width has been derived from equation (5) as a function of the radius R of the ferrite disks and the stripline width angle ψ (6) [2].

$$W = 2R \sin \psi \quad (5)$$

where

$$\psi = \frac{1}{\sqrt{3}} \frac{\pi(\kappa/\mu)}{1.84\sqrt{\mu_{eff}/\varepsilon}} \quad (6)$$

The effect of this geometric parameter on circulator performances has been studied in order to optimize the non-reciprocal component. Simulations with various values of the stripline width W have been performed (see Figure 4). The width W has been changed from 250 to 1200 μm . The insertion loss has reached the minimum value at $W = 400 \mu\text{m}$. After $W = 500 \mu\text{m}$ the insertion losses decreased rapidly.

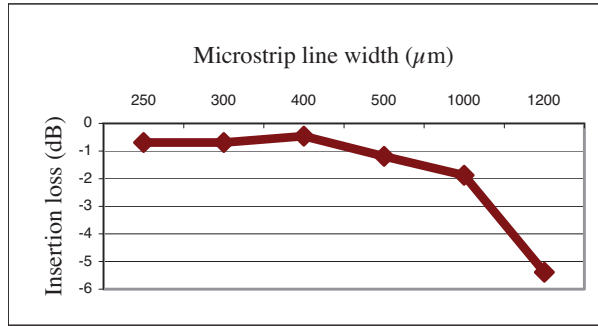


Figure 4. Numerical results for the insertion loss of a stripline circulator as a function of signal line width W .

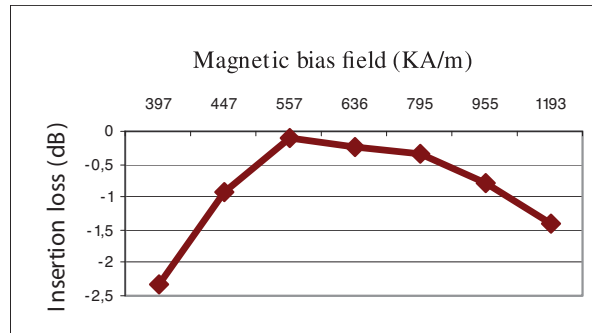


Figure 5. Numerical results for the insertion loss of our stripline circulator as a function of magnetic bias field H_i .

2.1.3. Effect of the Magnetic Bias Field H_i

The component is polarized and the internal magnetic field H_i in the YIG film is given by

$$H_i = H_{dc} + H_a - N_z M_s \quad (7)$$

Where H_{dc} is the external magnetic field ($H_{dc} = 636 \text{ kA/m}$, field that we can apply in our laboratory), H_a is the anisotropy field ($H_a = 0$ for the YIG), N_z is the demagnetizing factor ($N_z = 1$ for a thin film) and M_s is the saturation magnetization of the material. The obtained value of the internal magnetic field (H_i) is 557 kA/m which is uniformly applied to the YIG ferrite thin film.

In order to estimate the sensibility of losses up to the external bias field, we have made several simulations with different values of H_i .

Results are reported on Figure 5. The best value between 397 kA/m and 1193 kA/m is 557 kA/m. For this polarisation, insertion losses are better than -0.5 dB.

2.1.4. Comparison between Analytical and Numerical Results

To evaluate the performance of the circulator, we calculate the S -parameters of the dispersion matrix. In our case, the simple expression of the dispersion matrix is:

$$S = \begin{bmatrix} S_{11} & S_{31} & S_{21} \\ S_{21} & S_{11} & S_{31} \\ S_{31} & S_{21} & S_{11} \end{bmatrix} \quad (8)$$

It is now supposed that the coefficients of return loss (S_{11}), isolation (S_{31}) and insertion loss (S_{21}) referenced to port 1 are identical for port 2 and 3.

The S -parameters calculations are based on Neider's study [7] considering the losses in the conductor of the stripline circulator. The results from the analytical model are compared with the HFSS numerical results (see Figure 6).

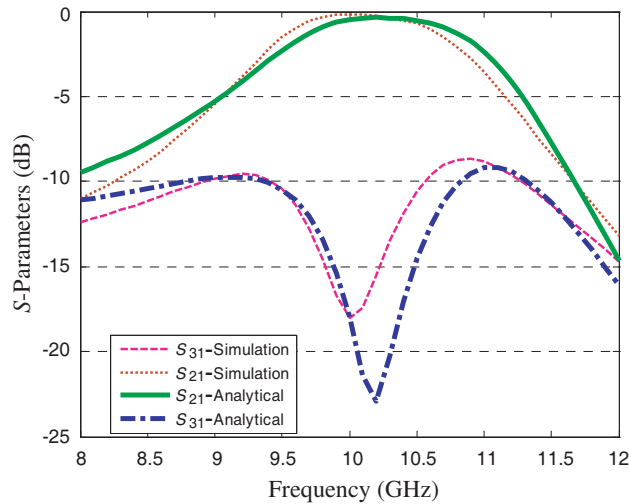


Figure 6. Evolution of S -parameters of the analytical and numerical study.

The levels of isolation and insertion loss obtained by simulation are equivalent to those obtained from the analytical model. However,

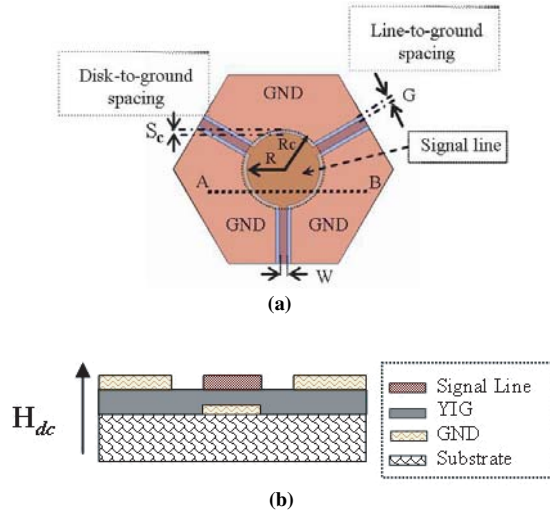


Figure 7. Structure of a circulator with CPW structure: (a) top view, (b) *A-B* cross-sectional of circulator with YIG thin film.

we can observe a little shift in frequency between the analytical and the numerical methods.

2.2. Transposing to Coplanar Circulator

The analytical and numerical experience must now be transposed onto a coplanar circulator design. The proposed structure of our circulator is shown in Figure 7. The circulator has a hexagonal shape and three ports (the impedance of each one is referenced to $50\ \Omega$) connected in a 120° *Y*-junction. The analytical values obtained from equations (5) and (6) for the stripline have been used to obtain the final design of the CPW structure. The radius of the inner conductor is $R = 2\ \text{mm}$ and the width of the access lines is $W = 400\ \mu\text{m}$ (Figure 7). A magnetic field (H_{dc}) is applied perpendicularly to the YIG film.

It is difficult to transpose the functioning of the stripline circulator into a coplanar design. To understand the reasons, Figure 8 shows the differences of field lines between the two technologies.

The electric and magnetic fields are shown in solid and broken lines, respectively. As shown in Figure 8(a), in stripline, signal line (Line) is placed between two ground (GND) planes. The electric field is stronger in the space sandwiched by the Line and the GND plane (vertical direction).

On Figure 8(b), CPW has the Line and the GND on the same

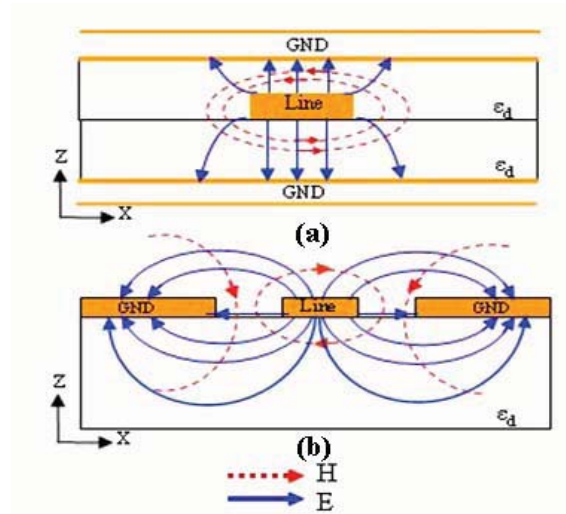


Figure 8. Schematic distribution of electric field (solid line) and magnetic field (dashed line) for (a) stripline and (b) CPW.

level with a small distance between them. The electric field shown in Figure 8(b) is stronger in the plane containing the Line and the GND (horizontal direction).

The considerations, of the previous paragraph, explain the stacking of the device presented on Figure 7(b). On a $635 \mu\text{m}$ thick of commercial alumina substrate (with the permittivity $\epsilon_r = 9.2$ and the dielectric loss tangent $\tan \delta = 6 \cdot 10^{-4}$ which are values given by the Neyco company at 9.8 GHz), a magnetic thin film is deposited. Then the signal line and the ground plane of the CPW are patterned on the magnetic film. From previous observation of the differences between the field of the stripline and the CPW, it is clear that in the central part of the device, the field must be modified. So, a metallic plane which is not connected to the GND is patterned under the central disk (Figure 7(b)). As the centre of the coplanar circulator is very similar to a microstrip structure, the field displacement between the centre conductor and the non-connected metallic plane facilitates the field transition between the line accesses and the centre of the circulator (see Figure 9).

To obtain the geometric parameters (the gap spacing for line accesses G , the disc to ground spacing S_c and the radius of the non-connected ground plane R_c), a numerical study is made to optimize the circulator performance.

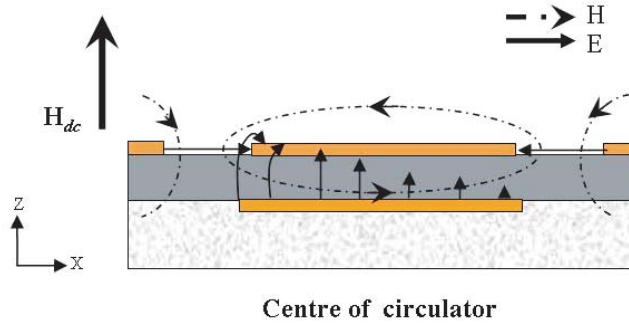


Figure 9. Field displacement in the centre of the circulator with coplanar junction

2.2.1. Effect of the G , S_c , and R_c

Several sets of simulation using Ansoft HFSS are carried out to estimate the behavior of the component. Three main parameters of the CPW are analyzed in order to quantify their effects on circulator performances.

The effect of Line-to-GND spacing G on transmission characteristic, such as insertion loss S_{21} and isolation S_{31} , has been studied. The structure under simulation has a $W = 400 \mu\text{m}$, a Disk-to-GND spacing (S_c) of $150 \mu\text{m}$, a radius of the lower non-connected ground plane (R_c) of 2.13 mm and a ferrite thickness of $20 \mu\text{m}$. The results are shown in Figure 10.

The parameters G is varied from 120 and $200 \mu\text{m}$, in the frequency band of circulation; insertion loss is around -2 dB and isolation is greater than 20 dB . As the circulator is designed to function at 10 GHz , we can say that best transmission properties are obtained for $G = 130 \mu\text{m}$ (see Figure 10(a)).

For the isolation value, the S_{31} parameter is lower than -30 dB (see Figure 10(b)). The frequency at which the best isolation is obtained seems to be influenced by the gap spacing. For $G = 120 \mu\text{m}$, this frequency is 10.06 GHz , and for $200 \mu\text{m}$, it becomes 9.96 GHz .

Another set of simulation is done to observe the effect of the Disk-to-GND spacing S_c on transmission characteristics (Figure 11). The simulation parameters are: a width of $400 \mu\text{m}$, a Line-to-GND spacing (G) of $130 \mu\text{m}$, a radius of the lower non-connected ground plane (R_c) 2.13 mm and a ferrite thickness of $20 \mu\text{m}$. Results are shown in Figure 11. The Disk-to-GND spacing S_c varied from 60 and $200 \mu\text{m}$. All structures give good results with insertion losses at -2 dB and with

an isolation better than -20 dB. The best insertion losses are obtained for $S_c = 200 \mu\text{m}$. As shown in the previous study, the effect of the parameter on insertion loss is not really important in the frequency band of interest. For $S_c = 200 \mu\text{m}$, isolation is better than -40 dB.

The last parameter is the radius of the lower non-connected ground plane (R_c). It is located between the ferrite and the dielectric substrate. The radius of this GND varies from 1.8 to 2.4 mm (as shown in Figure 12) the insertion loss reaches the minimum value at $R_c = 2.3$ mm. The S_{31} also reaches its best value for a radius of 2.3 mm (see Figure 12).

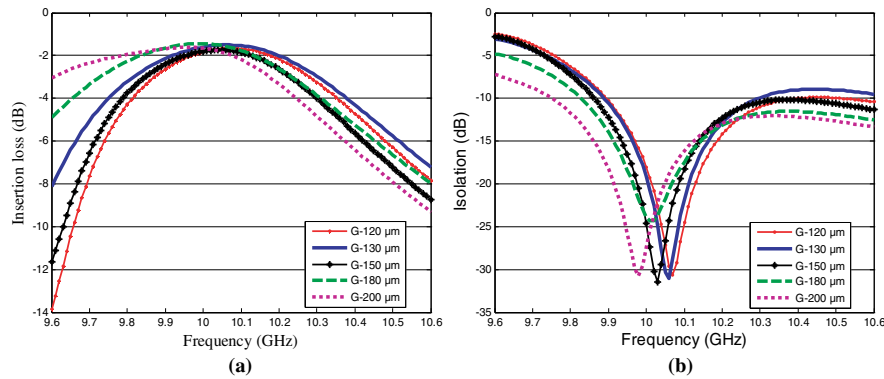


Figure 10. Dependence of S -parameters ((a) S_{21} , (b) S_{31}) with Line-to-GND spacing — G .

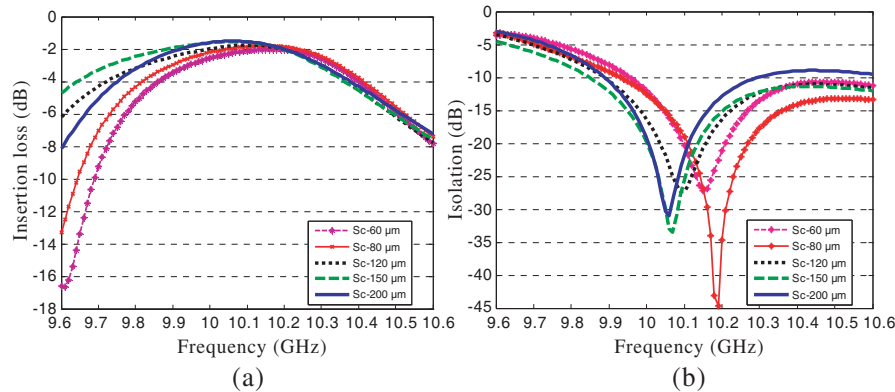


Figure 11. Dependence of S -parameters ((a) S_{21} , (b) S_{31}) with centre disk-to-GND spacing — S_c .

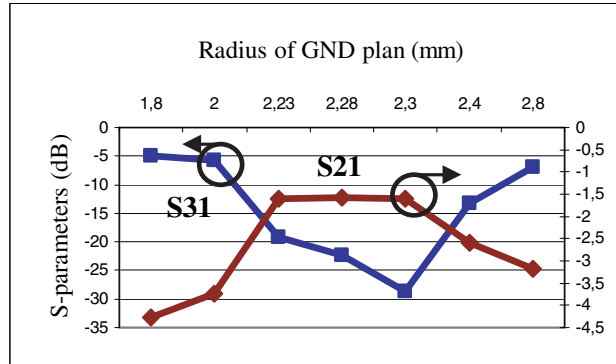


Figure 12. Dependence of S -parameters (S_{21} , S_{31}) on radius GND plane at 10 GHz.

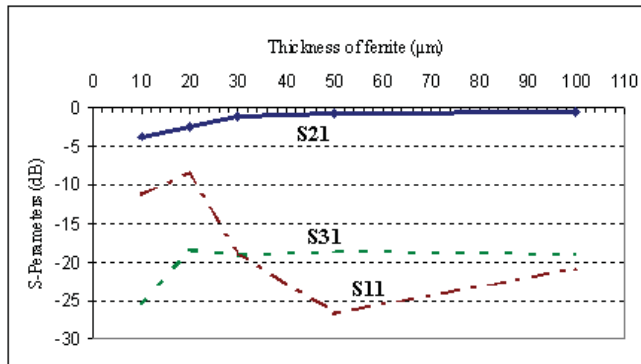


Figure 13. S -parameters (S_{21} , S_{31} , S_{11}) of a coplanar circulator as a function of the thickness of the ferrite.

2.2.2. Effect of the Thickness of the Ferrite

For different thicknesses of the YIG film, Figure 13 shows the performance of the circulator. The losses in the conductors are usually low compared to the magnetic and dielectric losses [7], but in our case the losses increase when the thickness of the ferrite decreases. For each set of parameters, an optimization process is realized, but we cannot argue that obtained results are the best ones for each structure. Therefore, we must be careful in analyzing the results of Figure 13. Nevertheless, the only characteristic which gives a regular variation is the “insertion losses”, thus we can conclude that the reduction of the ferrite thickness (from 100 μm to 10 μm) increases the losses

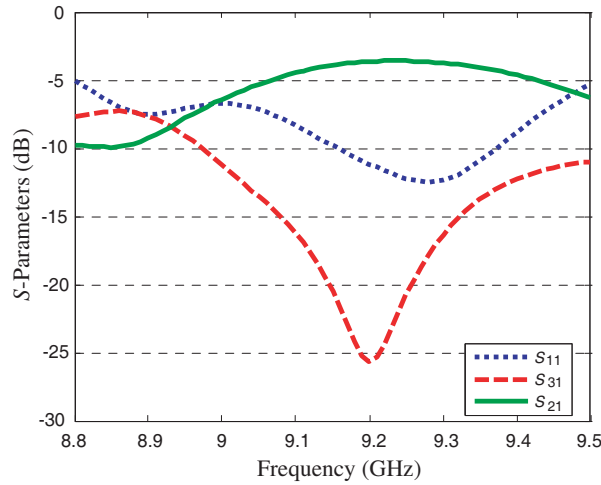


Figure 14. Frequency characteristics of S -parameters (insertion loss S_{21} , isolation S_{31} and return loss S_{11}) for a circulator with a $10\ \mu\text{m}$ ferrite YIG thin film.

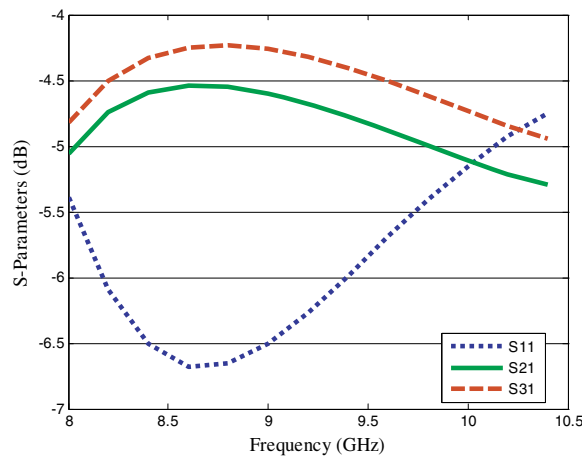


Figure 15. Frequency characteristics of S -parameters for a circulator with a $10\ \mu\text{m}$ ferrite YIG thin film in which GND plane under the ferrite is removed.

dramatically.

Figure 14 shows the frequency dispersion of S -parameters for a circulator with a $10\ \mu\text{m}$ YIG thin film. This is a very thin film compared to usual devices. Acceptable non-reciprocal transmission

characteristics are obtained at 9.20 GHz with -3.64 dB for insertion loss, isolation of -25.65 dB, and a bandwidth of 110 MHz (which is defined as the frequency where S_{31} is lower than -20 dB).

2.2.3. Effect of the Non-Connected Ground Plane

We have removed the non-connected GND plane which was located between the ferrite and the dielectric substrate in order to show its effect. The frequency dispersion of S -parameters of this circulator is presented in Figure 15. As it can be observed, the non-reciprocal transmission has disappeared.

3. CONCLUSION

A hexagonal circulator using a coplanar waveguide with Yttrium Iron Garnet ferrite has been designed using the theoretical results obtained by Bosma from a stripline structure which are transposed to a coplanar structure. The analytical study is completed by numerical analysis by using a 3-D finite element method simulator. Parametric studies enable to define the geometric parameters of a coplanar circulator and optimize the component's performance. The simulation results obtained for a circulator using $10\ \mu\text{m}$ YIG film are quite good (isolation of 25.65 dB at 9.2 GHz, insertion loss of 3.64 dB and bandwidth of about 110 MHz for a 20 dB isolation). Consequently, we proved that the fabrication of high frequency circulators using $10\ \mu\text{m}$ YIG film is possible. Of course some performances must be improved and some suggestions can be done. As an example, to reduce the insertion losses, some solutions can be explored such as changing the circulator shape of the central conductor to a triangular one [8, 9] or choosing other topologies, such as in [10].

REFERENCES

1. Bosma, H., "On the principle of stripline circulation," *Proc. Inst. Elec. Eng.*, Vol. 109, Pt. B, No. 21, 137–146, Jan. 1962.
2. Bosma, H., "On stripline Y -circulation at UHF," *IEEE Trans. Microwave Theory Tech.*, Vol. 12, 61–72, Jan. 1964.
3. Ogasawara, N. and M. Kaji, "Coplanar-guide and slot-guide junction circulators," *Electronics Letters*, Vol. 7, No. 9, 220–221, May 6, 1971.
4. Koshiji, K. and E. Shu, "Circulators using coplanar waveguide," *Electronics Letters*, Vol. 22, No. 19, 1000–1002, Sep. 11, 1986.

5. Oshiro, K., H. Mikami, S. Fujii, T. Tanaka, H. Fujimori, M. Matsuura, and S. Yamamoto, "Fabrication of circulator with coplanar wave-guide structure," *IEEE Trans. Magnetism*, Vol. 41, No. 10, 3550–3552, Oct. 2005.
6. Polder, D., "On the theory of electromagnetic resonance," *Phil. Mag.*, Vol. 40, 99, 1949.
7. Neidert, E. and P. M. Phillips, "Losses in Y-junction stripline and microstrip ferrite circulators," *IEEE Trans. Microwave Theory Tech.*, Vol. 41, No. 6/7, 1081–1086, Jun./Jul. 1993.
8. Helszajn, J., "Fabrication of very weakly and weakly magnetized microstrip circulators," *IEEE Trans. Microwave Theory and Tech.*, Vol. 46, 439–449, May 1998.
9. Bènevent, E., V. Larrey, D. Vincent, and A.-S. Dehlinger, "Losses origins in 10 GHz stripline circulator with 10 μm thick barium hexagonal ferrite films," *Proceedings of EuMC 2006*, Manchester, Sep. 10–15, 2006.
10. Didier, V., "Rectangular junction ferrite component in millimeter waves," *PIERS Online*, Vol. 4, No. 5, 526–530, 2008.